Association of Metallurgical Engineers of Serbia *Scientific paper*
AMES *UDC: 669.14.065.32*

DETERMINATION LHP OF AXISYMMETRIC TRANSIENT MOLYBDENUM STEEL-4037H QUENCHED IN SEA WATER BY DEVELOPING 1-D MATHEMATICAL MODEL

Abdlmanam S. A. Elmaryami*, Badrul Omar

University Tun Hussein Onn Malaysia, Mechanical Engineering Department
86400, Batu Pahat, Johor, Malasia

Received 18.01.2012
Accepted 04.04.2012

Abstract

The modelling of an axisymmetric industrial quenched molybdenum steel bar AISI-SAE 4037H quenched in sea water based on finite element method has been produced to investigate the impact of process history on metallurgical and material properties. Mathematical modelling of 1-dimensional line (radius) element axisymmetric model has been adopted to predict temperature history and consequently the hardness of the quenched steel bar at any point (node). The lowest hardness point (LHP) is determined. In this paper hardness in specimen points was calculated by the conversion of calculated characteristic cooling time for phase transformation t8/5 to hardness. The model can be employed as a guideline to design cooling approach to achieve desired microstructure and mechanical properties such as hardness. The developed mathematical model was converted to a computer program. This program can be used independently or incorporated into a temperature history calculator to continuously calculate and display temperature history of the industrially quenched steel bar and thereby calculate LHP. The developed program from the mathematical model has been verified and validated by comparing its hardness results with commercial finite element software results. The comparison indicates reliability of the proposed model.

Key words: Heat Treatment; Quenching; Axisymmetric Molybdenum Steel Bar; Finite Element; Mathematical Modeling; Unsteady State Heat Transfer.

Introduction

Quenching is a heat treatment usually employed in industrial processes in order to control mechanical properties of steels such as hardness [1, 2]. The process consists of raising the steel temperature above a certain critical value, holding it at that

* Corresponding author: Abdlmanam Elmaryami,damer604@yahoo.com

temperature for a specified time and then rapidly cooling it in a suitable medium to room temperature [1,3]. The resulting microstructures formed from quenching (ferrite, cementite, pearlite, upper bainite, lower bainite and martensite) depend on cooling rate and on chemical composition of the steel [1, 4].

Quenching of steels is a multi-physics process involving a complicated pattern of couplings among heat transfer. Because of the complexity, coupled (thermal-mechanical-metallurgical) theory and non- linear nature of the problem, no analytical solution exists. However, numerical solution is possible by finite difference method, finite volume method, and the most popular one - finite element method (FEM) [1, 5].

During the quenching process of the steel bar, the heat transfer is in an unsteady state as there is a variation of temperature with time [1, 6]. In this paper the heat transfer analysis will be carried out in 3- dimensions. The three dimensional analysis will be reduced into a 1-dimensional axisymmetric analysis to save cost and computer time [1, 5, 7-10]. This is achievable because in axisymmetric conditions the temperature deviations is only in r-direction while there is no temperature variation in the theta θ and z-direction as it is clear in Figs. 1-3. The Galerkin weighted residual technique is used to derive the mathematical model. In this work, 1-dimensional line (radius) element will be developed.

It is clear that the first point (node) will be completely cooled after quenching (surface node) because it is located on the surface touched by the cooling medium, then the other points (nodes) on the radial axis to the centre accordingly will be cooled and the last point will be completely cooled after quenching (centre node)[1].

It means that the maximum hardness will be measured on the surface node subjected to fast cooling, then the hardness will decrease from the surface node on the radial axis to the centre node of the quenched steel bar, respectively. This means that the lowest hardness point of the quenched steel bar will be detected at the centre node [1].

The lowest hardness point (LHP) should be expected inside the heat treated quenched steel bar at the half of the length at the centre of the bar (centre node). To prove this statement experimentally is an almost impossible task using manual calculation techniques. Also the earlier methods only used hardness value calculated at the surface (surface node), which is higher than the lowest hardness point (centre node). This might have negative consequences resulting to the deformation and failure of the component [1].

It will be more important to know the LHP (centre node) when the radius of the quenched steel bar will increase because the lowest hardness point will be lower than the hardness on the surface (surface node). This means that increasing the radius of the bar is inversely proportional to LHP (centre node), while the hardness at the surface (surface node) will be the same [1].

No published informations are available till date on this aspect. This paper represents a contribution towards understanding of steel behaviour at elevated temperature during quenching at the LHP (centre node) of the steel bar. We believe that the results of this paper might be very useful to obtain the hardness of the lowest point of the steel bar in order to reach the maximum benefit against the deformation and failure of the component [1].

Mathematical model

The temperature history of the quenched cylindrical molybdenum steel bar at any point will be calculated. Three dimensional heat transfers can be analyzed using one dimensional axisymmetric element as shown in Figs. 1-3. [34-39].

Methodology of building the Finite Element (FE) Model in details

The temperature distribution inside the cylindrical steel bar when reached thermal equilibrium will be calculated. There are special classes of three-dimensional heat transfer problem:

i. geometrically axisymmetric.
ii. each thermal load is symmetrical about an axis.

This 3-dimensional heat transfer problem may be analyzed using one-dimensional axisymmetric elements as shown in Figs. 1-3. [34-39].

The FE is applied to the 1-dimensional cylindrical coordinates heat transfer problem. The FE formulation is developed with the Garlekin Weighted-residual method. The appropriate working expressions of the conductance matrix, capacitance matrix and thermal load matrix are derived in details. The time dependent solution is obtained by applying the Backward Difference Schem.

Meshing the engineering problem of the domain

Let us consider a cylindrical molybdenum steel bar as shown in Fig. 1 which had been heated and then submerged in a cool quenching medium (sea water).

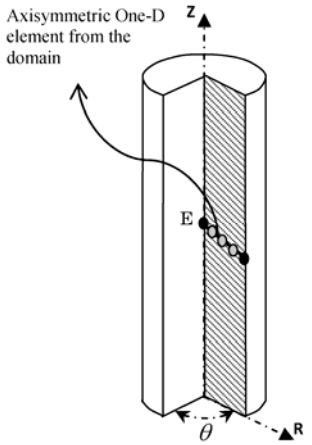

Fig. 1 The axisymmetric one dimensional line (radius) element from the domain, on the cylindrical molybdenum steel bar which had been heated and then quenched in sea water.

1-dimensional axisymmetric line (radius) element has been selected on this mathematical model. A 1-dimensional element in this work is defined by 5 nodes. Therefore, we can represent the variation of the dependent variable, such as the temperature history consequently the hardness at any point (node) even inside the heat treated quenched molybdenum steel bar.

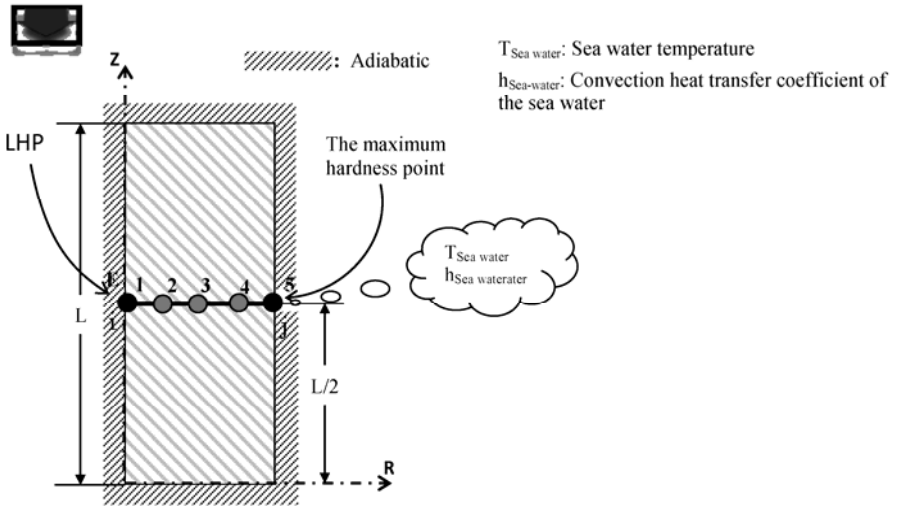

Fig. 2 The axisymmetric one dimensional line (radius) element from the domain on the axisymmetric rectangular cross-section.

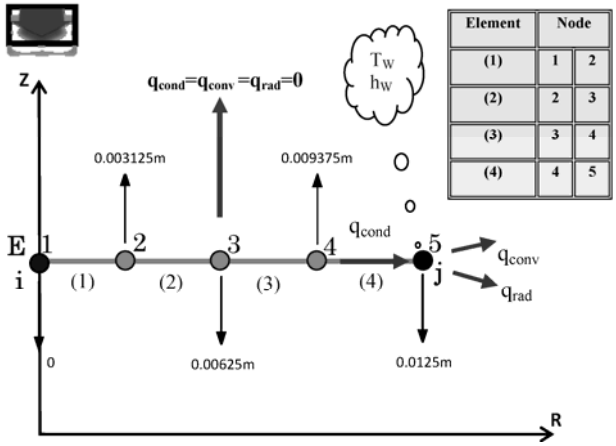

Fig. 3 The axisymmetric 1-dimensional line (radius) element from the domain shows the selected 4 elements with 5 nodes and the boundary at node j [5] for an element 4.

The linear temperature distribution for an element (radius) line, T is given by:

$$T^{(R)} = a_1 + a_2 R \qquad (1)$$

where: $T^{(R)}$ = nodal temperature as the function of R; a_1 and a_2 are constants, R is any point on the (radius) line element

Shape function of 1- dimensional axisymmetric element

The shape functions were to represent the variation of the field variable over the element. The shape function of axisymmetric 1-dimensional line (radius) element expressed in terms of the r coordinate and its coordinate are shown in Fig. 4; [34-39].

Global coordinate system being used to get the constants a_1 and a_2 thereby we can obtain the required shape function according to the below equations, which will be required for the Galerkin finite element solution.

$$S_i = \left(\frac{R_j - R}{R_j - R_i} \right) = \left(\frac{R_j - R}{L} \right) \quad (2a)$$

$$S_j = \left(\frac{R - R_i}{R_j - R_i} \right) = \left(\frac{R - R_i}{L} \right) \quad (2b)$$

Thus the temperature distribution of 1-dimensional radius for an element in terms of the shape function can be written as:

$$T^{(R)} = S_i T_i + S_j T_j = S^{(r)} \{T\} \quad (3)$$

Where $[S^{(r)}] = [S_i \quad S_j]$ is a row vector matrix and

$\{T\} = \begin{Bmatrix} T_i \\ T_j \end{Bmatrix}$ is a column vector of nodal temperature of the element.

Eq. (3) can also be expressed in matrix form as:

$$T_{(R)} = [S_i \quad S_j] \begin{Bmatrix} T_i \\ T_j \end{Bmatrix} \quad (4)$$

Thus for 1-dimensional element we can write in general:

$$\Psi^{(e)} = [S_i \quad S_j] \begin{Bmatrix} \Psi_i \\ \Psi_j \end{Bmatrix} \quad (5)$$

Where Ψ_i and Ψ_j represent the nodal values of the unknown variable which in our case is temperature. The unknown parameters can be deflection, velocity etc.

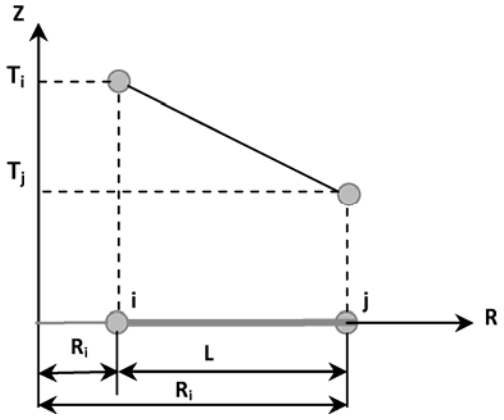

Fig. 4. 1-dimensional linear temperature distributions for an element (radius) line in Global Coordinate system.

Natural area coordinate

Using the natural length coordinates and their relationship with the shape function by simplification of the integral of Galerkin solution:

The two length natural coordinates L_1 and L_2 at any point p inside the element are shown in Fig. 5 from which we can write:

$$L_1 = \frac{R_j - R}{R_j - R_i} = \frac{l_1}{L} \tag{6a}$$

$$L_2 = \frac{R - R_i}{R_j - R_i} = \frac{l_2}{L} \tag{6b}$$

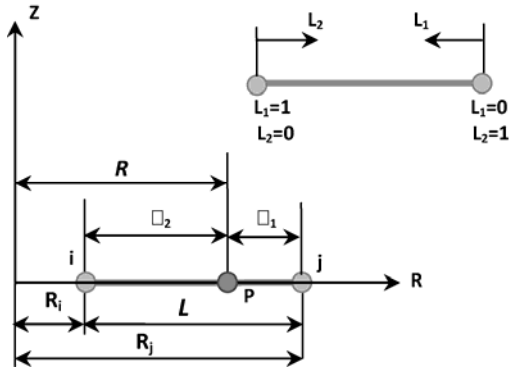

Fig. 5. Two-node line element showing interior point p and the two naturals coordinates L_1 and L_2.

Since it is a 1-dimensional element, there should be only one independent coordinate to define any point P. This is true even with natural coordinates as the two natural coordinates L_1 and L_2 are not independent, but are related as:

$$L_1+L_2 = 1 \quad or \quad L_1 + L_2 = \frac{l_1}{L} + \frac{l_2}{L} = 1 \tag{7}$$

The natural coordinates L_1 and L_2 are also the shape functions for the line element, thus:

$$S_i = \left(\frac{R_j - R}{R_j - R_i}\right) = \left(\frac{R_j - R}{L}\right) = L_1$$

$$S_j = \left(\frac{R - R_i}{R_j - R_i}\right) = \left(\frac{R - R_i}{L}\right) = L_2$$

$$S_i = L_1 , S_j = L_2, \tag{8}$$

$$R = R_j L_2 + R_i L_1 = R_i S_i + R_j S_j \tag{9}$$

$$\frac{\partial [S]_i}{\partial r} = \frac{\partial L_1}{\partial r} = \frac{-1}{R_j - R_i} = -\frac{1}{L} \tag{10}$$

$$\frac{\partial [S]_j}{\partial r} = \frac{\partial L_2}{\partial r} = \frac{1}{R_j - R_i} = \frac{1}{L} \tag{11}$$

Develop Equation for all Elements of the Domain

Derivation of equation of heat transfer in axisymmetric 1-dimensional line (radius) elements by applying the conservation of energy to a differential volume cylindrical segment has been done as shown in Fig. 6;

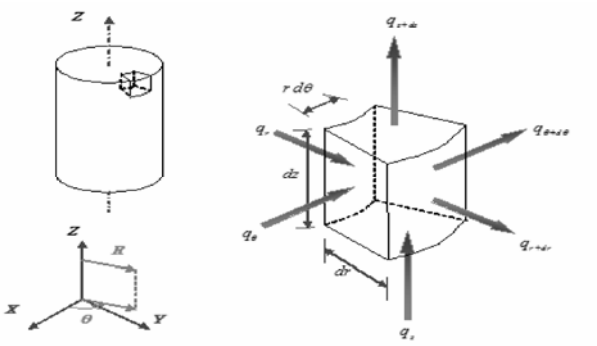

Fig. 6. Axisymmetric element from an axisymmetric body.

$$E_{in} - E_{out} + E_{generated} = E_{stored} \quad (12)$$

The transient heat transfer within the component during quenching can mathematically be described by simplifying the differential volume term [4, 11]; the heat conduction equation is derived and given by:

$$\frac{1}{r}\frac{d}{dr}\left(K_r r \frac{dT}{dr}\right) + \frac{1}{r^2}\frac{d}{d\theta}\left(K_\theta \frac{dT}{d\theta}\right) + \frac{d}{dz}\left(K_z \frac{dT}{dz}\right) + q = \rho c \frac{dT}{dt} \quad (13)$$

where:

k_r = heat conductivity coefficient in r-direction, W/m·°C.
k_θ = heat conductivity coefficient in θ-direction, W/m·°C.
kz = heat conductivity coefficient in z-direction, W/m·°C.
T = temperature, °C.
q = heat generation, W/m^3.
ρ = mass density, kg/m^3.
c = specific heat of the medium, J/kg·K.
t = time, s.

The Necessary Assumptions Made to Solve the Problem

i. For axisymmetric situations 1-dimensional line (radius) element, there is no variation of temperature in the Z-direction as shown in Figs. 1-3. This is because we have already assumed that in steel quenching and cooling process of the steel bar is insulated from convection at the cross section of the front and back.
   It means that we have convection and radiation at one node only which is on the surface [node 5]. In our research we focus to calculate LHP which is at [node 1], i.e. the last point that will be cooled. This gives the maximum advantage to make our assumption safer, because it is the last point that will be affected by convection and radiation from the front and back cross section of the steel bar. Therefore we can write, $\left(\frac{\partial T}{\partial z} = 0\right)$

For axisymmetric situations, there is no variation of temperature in the θ-direction, because it is clear from Figs. 1-3 that the temperature distribution along the radius will be the same if the radius move with angle θ, 360°. Therefore;

$$\left(\frac{\partial T}{\partial \theta} = 0 \right)$$

ii. The thermal energy generation rate $\dot{q}$ represents the rate of the conversion of energy from electrical, chemical, nuclear, or electromagnetic forms to thermal energy within the volume of the system. The conversion of the electric field will be studied in details in the second part of our research. Since in this manuscript no heat generation has been taken into account, therefore:

$$\dot{q} = 0$$

After simplifying, the Eq. (13) becomes;-

$$\frac{k}{r}\frac{\partial}{\partial r}\left(r \frac{\partial T}{\partial r} \right) = \rho \; c \frac{\partial T}{\partial t} \tag{14}$$

And also known as residual or partial differential equation:

$$\{\Re\} = \frac{k}{r}\frac{\partial}{\partial r}\left(r \frac{\partial T}{\partial r} \right) - \rho \; c \frac{\partial T}{\partial t} = 0 \tag{15}$$

Galerkin Weighted Residual Method Formulation

To suit the formulation into finite element analysis, Galerkin's weighted residual method is applied. The Galerkin residual in our case for 1-dimensional line (radius) element of unsteady state heat transfer can be obtained by integration the transpose of the shape functions times the residual which minimize the residual to zero becomes;

$$\int_V [S]^T \{\Re\}^{(e)} dv = 0 \tag{16}$$

Where, $[S]^T$ = the transpose of the shape function matrix

$\{\Re\}^{(e)}$ = the residual contributed by element (e) to the final system of equations.

$$\frac{k}{r}\int \overbrace{[S]^T \frac{\partial}{\partial r}\left(r \frac{\partial T}{\partial r} \right)}^{1} dv - \int \overbrace{[S]^T \rho c \frac{\partial T}{\partial t}}^{2} dv = 0 \tag{17}$$

Chain rule

The term 1 and 2 of Eq. (17) can be re-arranged using the chain rule which states that:

$$(fg)^- = fg^- + gf^-$$

Therefore, $fg^- = (fg)^- - f^- g$ then $\frac{\partial}{\partial r}\left([S]^T r \frac{\partial T}{\partial r} \right) = [S]^T \left\{ \frac{\partial}{\partial r}\left(r \frac{\partial T}{\partial r} \right) \right\} + r \frac{\partial T}{\partial r} \frac{\partial [S]^T}{\partial r}$

Term 1 of Eq. 17 is rearranged, thus:

$$[S]^T\left\{\frac{\partial}{\partial r}\left(r\frac{\partial T}{\partial r}\right)\right\} = \frac{\partial}{\partial r}\left([S]^T r\frac{\partial T}{\partial r}\right) - r\frac{\partial T}{\partial r}\frac{\partial [S]^T}{\partial r} \tag{18}$$

By substitute Eq. (18) into Eq. (17):

$$= \overbrace{\frac{k}{r}\int\left\{\frac{\partial}{\partial r}\left([S]^T r\frac{\partial T}{\partial r}\right)\right\}dv}^{A} - \overbrace{\frac{k}{r}\int\left\{\frac{\partial [S]^T}{\partial r} r\frac{\partial T}{\partial r}\right\}dv}^{B} - \underbrace{\int [S]^T\left\{\rho\, c\,\frac{\partial T}{\partial t}\right\}dv}_{C} \tag{19}$$

Term A is the heat convection term and contributes to the conductance and thermal load matrix. Term B is the heat conduction term and contributes to the conductance matrix. Term C is the transient equation and contributes to the capacitance matrix.

Where: $\overbrace{\frac{k}{r}\int\frac{\partial}{\partial r}\left([S]^T r\frac{\partial T}{\partial r}\right)dV}^{A} = \underbrace{-2\pi hrz\,[S]^T[S]\{T\}^e}_{A_1} + \underbrace{2\pi hrz\,[S]^T T_f}_{A_2} -$

$\underbrace{2\pi rz\,\varepsilon_s\sigma\,[S]^T[S]\{T\}^e\left([S]\{T\}^e\right)^3}_{A_3} + \underbrace{2\pi rz\,\varepsilon_s\sigma\,[S]^T T_f^4}_{A_4}$

Note that terms A_1 and term A_3 contributed to the conductance matrix since they contains the unknown temperature {T}. Terms A_2 and A_4 contributed to the thermal load matrix as T_f is the known fluid temperature. Terms A_3 and term A_4 refer to heat radiation and are very important if our heat treatment is Annealing [cooling in the furnace] or Normalizing [cooling in air or jet air], but they can be ignored if cooling is quenching in sea water as in our work.

From earlier explanations derivation and after simplification we can formulate the conductance matrix in the r-direction for term B. Finally we get:

Term B (the conduction term) contributes to the Conductance Matrix

$$\overbrace{\frac{k}{L}\left(R_j - R_i\right)\begin{bmatrix}1 & -1\\ -1 & 1\end{bmatrix}\begin{Bmatrix}T_i\\ T_j\end{Bmatrix}}^{K_c} \tag{20}$$

Similarly, term C, the unsteady state (transient) which contributes to the Capacitance Matrix, becomes:

Term C (heat stored) contributes to the Capacitance Matrix

$$\overbrace{\frac{L\rho c}{6}\begin{bmatrix}\left(3R_i + R_j\right) & \left(R_i + R_j\right)\\ \left(R_i + R_j\right) & \left(R_i + 3R_j\right)\end{bmatrix}\begin{Bmatrix}T_i\\ T_j\end{Bmatrix}}^{C} \tag{21}$$

Term A (Heat Convection)

→ Term A_1 -Contributes to Conductance Matrix

Term A_1 *(the convection term) contributes to the conductance matrix*

$$\underbrace{-2hR_j\begin{bmatrix}0 & 0\\ 0 & 1\end{bmatrix}\begin{Bmatrix}T_i\\ T_j\end{Bmatrix}}_{K_h} \tag{22}$$

→ Term A_2 -Contributes to Thermal Load Matrix

Term A2 (the convection term) contributes to thermal load matrix

$$\underbrace{2hR_jT_w\begin{bmatrix}0\\ 1\end{bmatrix}}_{f_h} \tag{23}$$

Construct the element Matrices to the Global Matrix

The global, conductance, capacitance and thermal load matrices and the global of the unknown temperature matrix for all the elements in the domain are assembled i.e. the element's conductance; capacitance and thermal load matrices have been derived. Assembling these elements is necessary in all FE analysis.

Constructing these elements will result into the following FE equation:

$$[K]^{(G)}\{T\}^{(G)} + [C]^{(G)}\{\dot{T}\}^{(G)} = \{F\}^{(G)} \tag{24}$$

where:

[K]=[Kc]+[Kh]: is conductance matrix due to Conduction (Elements 1 to 4) and heat loss through convection at the element's boundary (element 4 node 5) as shown in Figs. 1-3.

{T}: is temperature value at each node, °C.

[C]: is capacitance matrix, due to transient equation (heat stored)

$\{\dot{T}\}$: is temperature rate for each node, °C/s.

$\{F\} = \{F_h\} + \{F_{\dot{q}}\}$: is heat load due to heat loss through convection at the element's boundary (element 4 node 5) and internal heat generation (element 4 node 5).

Euler's method

Two point recurrence formulas will allow us to compute the nodal

temperatures as a function of time. In this paper, Euler's method which is known as the backward difference scheme (FDS) will be used to determine the rate of change in temperature, the temperature history at any point (node) of the steel bar [4, 11-14].

If the derivative of T with respect to time t is written in the backward direction and if the time step is not equal to zero ($\Delta t \neq 0$), then we have:

$$\left\{\dot{T}\right\} \approx \left\{\frac{T(t)-T(t-\Delta t)}{\Delta t}\right\} \tag{25}$$

With;

$\{\dot{T}\}$= temperature rate (°C/s); T (t)= temperature at (t) s (°C); T (t - Δt) = temperature at (t - Δt) s, (°C)

Δt = selected time step (s) and t = time (s) (at starting time, t = 0)

By substituting the value of $\{\dot{T}\}$ into the finite element global equation, we obtain:

$$[K]^{(G)}\{T(t)\}^{(G)} + [C]^{(G)}\left\{\frac{T(t)-T(t-\Delta t)}{\Delta t}\right\}^{(G)} = \{F(t)\}^{(G)} \tag{26}$$

Finally, the matrices become;

$$\left[[K]^{(G)}\Delta t + [C]^{(G)}\right]\{T\}_{i+1}^{(G)} = [C]^{(G)}\{T\}_{i}^{(G)} + \{F\}_{i+1}^{(G)}\Delta t \tag{27}$$

From Eq. (27) all the right hand side is completely known at time t, including t = 0 for which the initial condition apply.

Therefore, the nodal temperature can be obtained for a subsequent time given the temperature for the preceding time.

Once the temperature history is known the important mechanical properties such as hardness and strength of the molybdenum steel bar can be obtained.

Application

Calculation the temperature history

The present developed mathematical model is programmed using MATLAB to simulate the results of the temperature distribution with respect to time in transient state heat transfer of the industrial quenched molybdenum steel bar.

The cylindrical molybdenum steel bar has been heated to 850°C. Then being quenched in sea water with $T_{sea\text{-}water}$ = 32°C and convection heat transfer coefficient, $h_{sea\text{-}water}$ = 1250 W/m^2·°C [15]. The temperature history for the selected nodes of the cylindrical molybdenum steel bar after quenching is being identified in Figs. 7 and 8. The cylindrical bar was made from molybdenum steel, with properties as mentioned below.

Thermal capacity, ρc (J/m3·°C):

$0 \le T \le 650$ °C, $\rho c = (0.004\ T + 3.3) \times 10^6$, $650 < T \le 725$ °C,

$\rho c = (0.068\ T - 38.3) \times 10^6$

$725 < T \le 800$ °C, $\rho c = (-0.086\ T + 73.55) \times 10^6$, $T > 800$ °C,

$\rho c = 9.55 \times 10^6$

Thermal conductivity, k (W/m·°C):

$0 \le T \le 900$ °C, $k = -0.022\ T + 48$, $T > 900$ °C, $k = 28.4$

In our case Eq. (27) becomes:

$$[K]^{(G)}\{T\}^{(G)} + [C]^{(G)}\{\dot{T}\}^{(G)} = \{F\}^{(G)}$$

And their respective equations:

$$[K]^{(G)} = [K_c]^{(1)} + [K_c]^{(2)} + [K_c]^{(3)} + [K_c]^{(4)} + [K_h]^{(4)} \quad (28)$$

$$[C]^{(G)} = [C]^{(1)} + [C]^{(2)} + [C]^{(3)} + [C]^{(4)} \quad (29)$$

$$\{F\}^{(G)} = \{F_h\}^{(4)} \quad (30)$$

With the input data and boundary conditions provided, a sensitivity analysis is carried out with the developed program to obtain the temperature distribution at any point (node) of the quenched steel bar. As an example, is the transient state temperature distribution results of the selected five nodes from the center [W_1] to the surface [W_5] of the quenched steel bar which were computed as shown in Figs. 7 and 8.

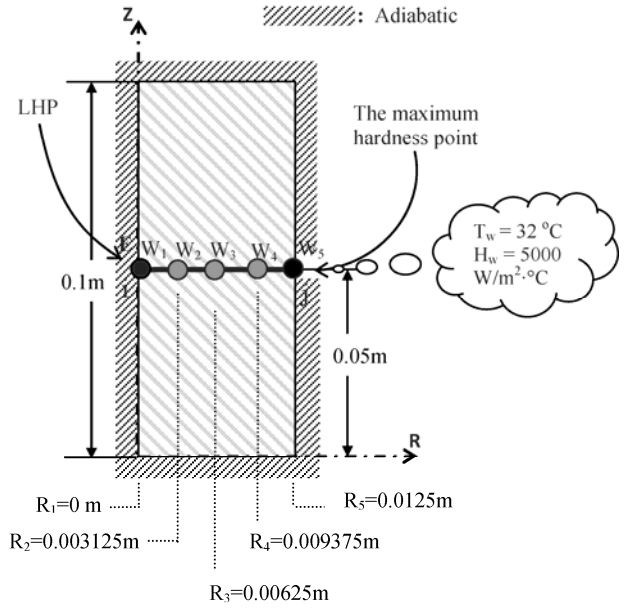

Fig. 7 The axisymmetric 1-dimensional line (radius) element from the domain when the radius equals 12.5mm, the selected 4 elements with 5 nodes and the boundary at node j [5] for an element 4.

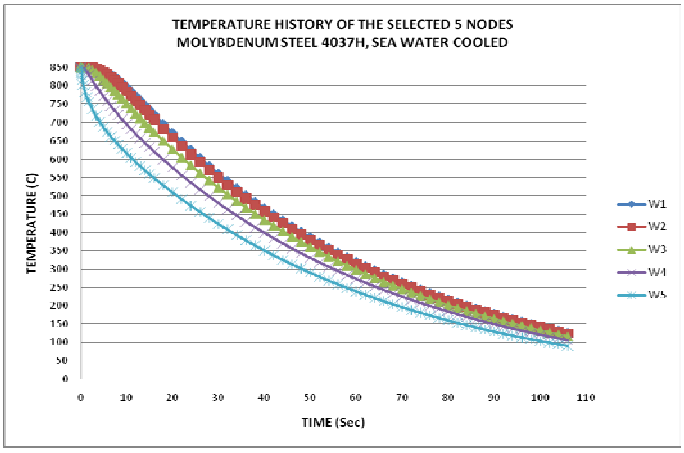

Fig. 8 Graph of temperature history along WW cross-section from MATLAB program.

LHP Calculation

Calculating the cooling time required

In this study, we choose to calculate the cooling time between 800°C and 500°C [11, 20-26]. Where, the characteristic cooling time, relevant for phase transformation in most structural steels is the time of cooling from 800 to 500°C (time $t_{8/5}$) [7-10, 27-34].

$t_c = t_{800} - t_{500}$

From Fig. 8 we can determine the time taken for node W_1 to reach 800°C,

$t_{800} = 9.7$ s.

By the same way the time taken for node W_1 to reach 500°C is

$t_{500} = 36.3$ s.

So the Cooling time tc for node W_1;

$t_c = t_{500} - t_{800} = 36.3 - 9.7 = 26.60$ s.

For nodes W_2 to W_5, the cooling time t_c was calculated by the same way, the final results are shown in Table 1.

Calculating the Jominy distance from Standard Jominy distance versus cooling time curve

Obtained cooling time, t_c, will now be substituted into the Jominy distance versus cooling time curve in order to obtain the correspondent Jominy distance. Jominy distance can also be calculated by using polynomial expressions via polynomial regression via Microsoft Excel.

In this paper the standard Table [Cooling rate at each Jominy distance (Chandler, H., 1998)] will be used [33]. Then Jominy distance of nodes W_1 to W_5 will be calculated by using the data from [Cooling rate at each Jominy distance (Chandler, H., 1998)], the final results are shown in Table 1, where the rate of cooling (ROC) was defined by:

$$\mathrm{ROC} = \frac{800°\mathrm{C} - 500°\mathrm{C}}{t_c} = \frac{800°\mathrm{C} - 500°\mathrm{C}}{t_{500°\mathrm{C}} - t_{800°\mathrm{C}}} \ (°\mathrm{C/s})$$

Predict the hardness of the quenched steel bar

The Rockwell hardness C (HRC) of molybdenum steel AISI-SAE 4037H can be calculated by using the relation between the Jominy distance and the HRC from the Practical date Handbook, the Timken Company 1835 Duebex Avenue SW Canton, Ohio 44706-2798 1-800-223. The final results are shown in Fig. 9 and Table 1.

Table 1 Cooling time, cooling rate, Jominy distance and HRC for the nodes W_1 to W_5, sea water cooled.

Node	t_c (s)	ROC (°C /s)	Jominy-distance (mm)	Hardness (HRC)
W_1	26.61	11.273957	16.735	23.909
W_2	26.571	11.290504	16.717	23.919
W_3	26.183	11.457816	16.479	24.066
W_4	24.546	12.221950	15.639	24.652
W_5	20.466	14.658457	14.159	25.624

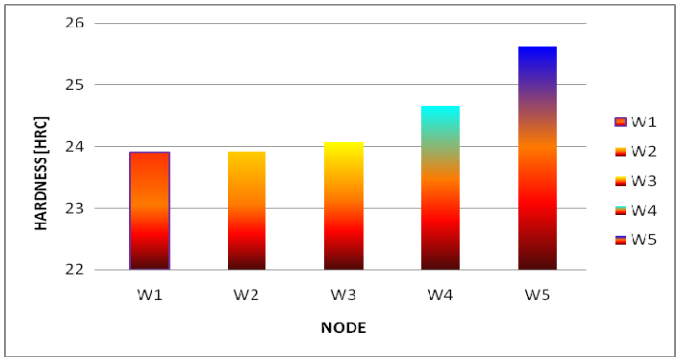

Fig. 9. Hardness distribution along WW cross-section for the nodes W_1 to W_5 from the centre to the surface, respectively, at half the length at the centre of the quenched steel bar.

Mathematical verification

The same data input for the steel properties and boundary condition used in the mathematical model was applied to the ANSYS software to verify the temperature simulation results. The temperature distribution from the ANSYS analysis is depicted figuratively as shown in Figs. 10.1a and 10.1b.

Fig. 10.1a shows the temperature distribution just before the steel bar becomes completely cooled whereas Fig. 10.1b shows the temperature distribution at the moment when the entire steel bar becomes completely cooled after 1498s.

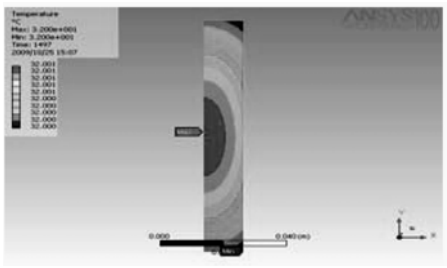

Fig. 10.1a

Fig.10.1b

The temperature time graph from the ANSYS analysis is depicted as shown in Fig. 11.

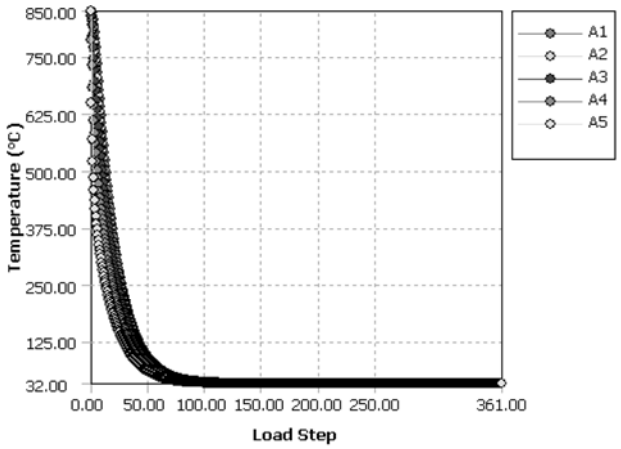

Fig. 11 Temperature-time graph from ANSYS

From the graphs shown in Fig. 8 (applied mathematical model) and Fig. 11 (applied ANSYS), it can be clearly seen that the temperature history of the quenched steel bar has the same pattern. The heat transfer across the steel bar is uniform. From Fig. 11 the cooling time, Jominy-distance and consequently the hardness of the quenched molybdenum steel 4037H at any point (node), even the (LHP) are also determined by ANSYS. The final results are shown in Table 2 and Fig. 12.

Table 2 Cooling time, cooling rate, Jominy distance and HRC for the nodes A_1 to A_5, determined by ANSYS.

Node	Cooling time,	Cooling rate	J-distance (mm)	HRC
A_1	32.112284	9.34222	18.788	22.668
A_2	32.030048	9.36621	18.763	22.684
A_3	31.466551	9.53393	18.590	22.795
A_4	28.484752	10.53195	17.677	23.380
A^5	24.074572	12.46128	15.468	24.759

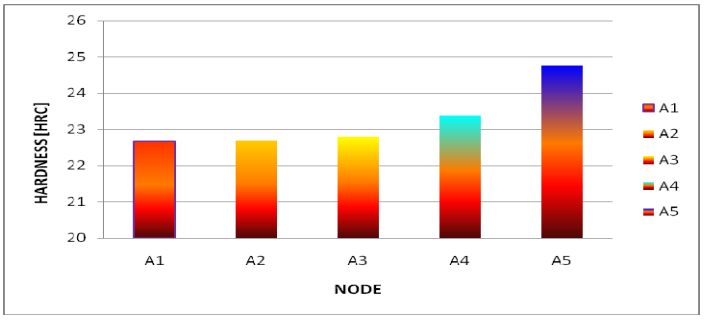

Fig. 12 Hardness distribution by ANSYS along AA cross section for the nodes A_1 to A_5 from the centre to the surface respectively at half the length at the centre of the quenched molybdenum steel bar.

From our results we found that in the mathematical model for the first node with W_1 in the center, we found that HRC = 23.909. While in ANSYS for the same node A_1, we found that HRC = 22.668.

And for the nodes on the surfaces W_5 and A_5, it was found that HRC = 25.624 and 24.759 for the mathematical model and ANSYS respectively. From the above, it can be seen that there is a strong agreement between both results. The difference between all the results of the mathematical model and the ANSYS simulations can be accounted due to the fact that the ANSYS software is for the commercial purpose, and thereby has some automated input data. But the developed mathematical model is precisely for a circular steel bar axisymmetric cross section. However, there is strong agreement between both results and thereby the result is validated where, the comparison indicated reliability of the proposed model. Also the results showed that the node on the surface will be the first which was completely cooled after quenching because it was in the contact with the cooling medium. The other nodes on the radial axis to the centre were successively cooled. The last point that would be completely cooled will be located at half the length of the centre. Hence, LHP will be at half the length of the centre of the quenched industrial molybdenum steel bar. It will be more important to know LHP once the radius of the quenched steel bar is large because LHP will be low. In other words, it will be lower than the hardness at the surface. This means that increasing the radius of the bar is inversely proportional with LHP. LHP calculation experimentally is an almost impossible task using manual calculation techniques also the earlier methods only used hardness calculated at the surface, which is higher than LHP, but this might have negative consequences resulting to deformation and failure of the component.

Conclusion

A mathematical model of steel quenching has been developed to compute LHP of the quenched molybdenum steel 4037H at any point (node) in a specimen with cylindrical geometry. The model is based on the finite element Galerkin residual method. The numerical simulation of quenching consisted of numerical simulation of temperature transient field of cooling process. This mathematical model was verified

and validated by comparing the hardness results with ANSYS software simulations. From the mathematical model and ANSYS results, it is clear that the nodes at the surface [W_5 and A_5], respectively, cool faster than the nodes at the center [W_1 and A_1], respectively, because t_{CW5} is less than t_{CW1} and t_{CA5} is less than t_{CA1}. This means that the mechanical properties such as hardness will be different, i.e. the hardness at the surface nodes [W_5 and A_5] will be higher than the hardness at the center nodes [W_1 and A_1].

Acknowledgement

The authors would like to thank the Ministry of Science, Technology and Innovation, Malaysia, for supporting this research under the Science Fund Grant with grant number {03-01-13-SF0071}.

The corresponding author is grateful to the Postgraduate Centre of UTHM for their supported this research where, they accepted him under the university PhD scholarship.

References

[1] Abdlmanam S. A. Elmaryami and Badrul Omar, (2011). "Unsteady State Computer Simulation of 2 Chromium Steel at 925°C as Austenitizing Temperature to Determine LHP". Metalurgia-Journal of Metallurgy [MJoM].

[2] M. Robert K. N., "Quenching and Tempering of Welded Steel Tubular". The Fabricator articles, 2001.

[3] Badrul Omar, Mohamed Elshayb and Abdlmanam S. A. Elmaryami: In: 18th world IMACS-MODSIM Congress, Cairns, Australia 2009, Proceedings, p. 1699–1705, 2009, SCOPUS indexed.

[4] Elshayeb Mohamed & Yea Kim Bing, Application of finite difference and finite element methods, University Malaysia Sabah Kota Kinabalu, 2000.

[5] Abdlmanam S. A. Elmaryami and Badrul Omar, "Developing of Unsteady State Axi-symmetric FEMM to Predict the Temperature of Industrial Quenched Steel" (2011), Journal of Metals Science and Heat Treatment, [Impact Factor 0.34],

[6] Budinski, K. G. (1992). "Engineering Material: Properties and Selection." 4th ed. Prentice-Hall International. Inc. 285-309.

[7] Abdlmanam S. A. Elmaryami, Heat treatment of steel by developing finite element mathematical model and by simulation. Master's thesis. University Tun Hussein Onn, Malaysia, 2010.

[8] Abdlmanam S. A. Elmaryami and Badrul Omar, "Developing 1-D MM of Axisymmetric Transient Quenched Boron Steel to Determine LHP". European Journal of Scientific Research, 2011. [Impact factor, [0.43, 2010]

[9] Abdlmanam S. A. Elmaryami and Badrul Omar, "Computer Simulation to Predict the Hardness of Transient Axi-Symmetric Industrial Quenched Steel Bar at Different Radial Axises" International Journal of Emerging Technologies in Sciences and Engineering, 2011.

[10] Abdlmanam S. A. Elmaryami and Badrul Omar, "Transient Computer Simulation of Industrial Quenched Steel Bar to Determine LHP of Molybdenum and Boron Steel at 850°C as Austenitizing Temperature Quenched in Different Medium" International Journal of Material Science, 2011.

[11] Saeed Moaveni, Finite element analysis; theory and application with ANSYS, Pearson education international, USA, 2008.
[12] Fuhrmann, J, and Hömberg, D., Numerical Simulation of the Surface Hardening of Steel. International Journal of Numerical Methods for Heat & Fluid Flow, (1999) 9(6):705-724.
[13] Chandler, H., Hardness Testing Applications. Hardness Testing Second Edition: 111-133. United States of America: ASM International, 1999.
[14] Saeed Moaveni, Finite Element Analysis. A Brief History of the Finite Element Method and ANSYS. 6-8.Pearson Education, Inc, USA, 2003.
[15] Film coefficient of water (h) is provided by Steel Industries (Sabah) Sdn Bhd, Malaysia and it is dependent upon the surface temperature of steel bar. Since h is provided, hence, has simplified the convection of cooling chamber without considering the complicated nature of forced convection.
[16] P.M.Unterweiser, H.E.Boyer and J.J.Kubbs, Heat Treaters Guide: Standard Practice and Procedure for Steel, eds, ASM, Metals Park, Ohio, (1982). (UCD PSL: TN751.H4 1982 (REF)).
[17] Properties of alloy steel AISI 50B46H, http://www.efunda.com/Materials/ CA 94088, Copyright © 2009 eFunda eFunda..
[18] ASM, "Properties and Selection: Irons, Steels, and High-Performance Alloys," Tenth Edition, Vol. 1, Heat Treating, American Society for Metals, 1990.
[19] Budinski, K. G., "Engineering Material: Properties and Selection." 4th ed. Prentice-Hall International. Inc. 285-309, 1992.
[20] Abdlmanam. S. A. Elmaryami, Sulaiman Bin Haji Hasan, Badrul Omar, Mohamed Elshayeb, Unsteady State Hardness Prediction of Industrial Quenched Steel Bar [One and Two Dimensional], Journal of Materials Science and Technology, 2009.
[21] A. Rose et al, Atlas zur Wärmebe- handlung der Stähle I, Verlag Stahleisen, Düsseldorf, 1958.
[22] Bozo, S., "Numerical Simulation of As-quenched Hardness in a Steel Specimen of Complex Form. Communications in Numerical Method in Engineering", 1998 14. 277-285.
[23] Abdlmanam S. A. Elmaryami and Badrul Omar, "LHP CALCULATION BY DEVELOPING MM OF AXISYMMETRIC TRANSIENT QUENCHED BORON STEEL, SEA WATER COOLED". International Journal of Engineering Science and Technology (IJEST™), 2011, [Impact Factor 1.85 in 2009, Index Copernicus (IC Value)-3.14, 2011-12]
[24] Abdlmanam S. A. Elmaryami, Sulaiman Bin Haji Hasan, Badrul Omar and Mohamed Elshayeb, "Unsteady state hardness prediction of industrial quenched steel bar [one and two dimensional]". Materials Science and Technology Conference and Exhibition, (MS & T'09), October 25-29, 2009, David L. Lawrence Convention Centre, Pittsburgh, Pennsylvania, USA, ISBN: 978-161567636-1, vol. 3, 2009, p. 1514–1520, Code 79396, SCOPUS indexed.
[25] Abdlmanam.S.A.Elmaryami, Badrul Omar and Mohamed Elshayeb, 5th European Metallurgical Conference, Innsbruck, Austria, 2009, volume 4, p. 1492-1495
[26] B. Smoljan: In: 13th International Science Conference, The Polish Academy of Science, Poland, 2004.

[27] B. Smojan (2006). Prediction of mechanical properties and microstructure distribution of quenched and tempered steel shaft, journal of materials processing technology, volume 175, Issu1-3, p. (393-397).

[28] B. Donnay, J. C Herman and V.Leroy (CRM, Belgium) U. Lotter, R. Grossterlinden and H. Pircher (Thyssen Stahl AG, Germany), Microstructure Evolution of C-Mn Steel in the Hot Deformation Process: The Stripcam Model.

[29] Bozidar Liscic (2010) System for process Analysis and hardness prediction when quenching Axially-Symmetrical workpieces of any shape in liquid quenchants, Journal of materials science form (vol. 638-642).

[30] B. Smoljan, D. Iljkić, S. Smokvina Hanza, Computer simulation of working stress of heat treated steel specimen, Journal of Achievements in Materials and Manufacturing Engineering 34/2 (2009) 152-156.

[31] Hsieh, Rong-Iuan; Liou, Horng-Yih; Pan, Yeong-Tsuen (2001), Effect of cooling time and alloying elements on the microstructure of the gleeble-simulated heat-affected zone of 22% Cr duplex stainless steels, journal of materials engineering and performance, volume 10, ssue 5, pp. 526-536.

[32] Croft, D.R. 1989. Thermal Analysis of An Industrial Heat Treatment Problem. Proceedings of the Sixth International Conference held in Swansea, UK on July 3rd-July 7th 1989, Numerical Methods in Thermal Problems Volume VI, Part 2 1813:1822.

[33] Chandler, H. 1999. Hardness Testing Applications. Hardness Testing Second Edition: 111-133. United States of America: ASM International.

[34] Abdlmanam S. A. Elmaryami and Badrul Omar, "Modeling the lowest hardness point in steel bar during quenching". Journal of ASTM International, Vol. 9, 2011, No. 5, ID JAI104386. [Impact Factor 0.279].

[35] Abdlmanam S. A. Elmaryami and Badrul Omar, "Developing 1-D MM of Axi-symmetric Transient Quenched Cr-Steel to Determine LHP, water cooled". Journal of Metallurgy Volume 2012 (2012), Article ID 539823, 9 pages doi:10.1155/2012/539823, http://www.hindawi.com/journals/jm/2012/539823/

[36] Abdlmanam S. A. Elmaryami and Badrul Omar, "Effect of Radius on Temperature History of Transient Industrial Quenched Cr-Steel 8650H by Developing 1-D MM". Journal of Applied Mathematical Sciences, 2011, [Impact Factor 0.275].

[37] Abdlmanam S. A. Elmaryami and Badrul Omar, "Developing 1-D MM of Axi-symmetric Transient Quenched Mo-STEEL AISI-SAE 4037H to Determine LHP". Journal of Metallurgy and Materials Science, Vol. 53, 2011, No. 3, P. 289-303. http://www.indianjournals.com/ijor.aspx?target=ijor:jmms&volume=53&issue=3&article=008

[38] Abdlmanam. S. A. Elmaryami and Badrul Omar, "Determination LHP of axisymmetric transient industrial quenched chromium steel 8650H by developing 1-D MM, sea water cooled". International Journal of Applied Engineering Research, 2011, [impact factor: 2].

[39] Abdlmanam S. A. Elmaryami and Badrul Omar, "The lowest hardness point calculation by transient computer simulation of industrial steel bar quenched in oil at different austenitizing temperatures". International Conference on Management and Service Science, MASS, Wuhan, China, Article number 5999335, Indexed by Ei Compendex, Sponsors: IEEE. SCOPUS indexed.